51st IEEE Conference on Decision and Control
December 10-13, 2012. Maui, Hawaii, USA

A Numerical Algorithm for Nonlinear $\mathcal{L}_2$-gain Optimal Control With Application to Vehicle Yaw Stability Control

Vladimir Milić* , Stefano Di Cairano**, Josip Kasać, Alberto Bemporad, and Željko Šitum

***Abstract*— This paper is concerned with $\mathcal{L}_2$-gain optimal control approach for coordinating the active front steering and differential braking to improve vehicle yaw stability and cornering control. The vehicle dynamics with respect to the tire slip angles is formulated and disturbances are added on the front and rear cornering forces characteristics modelling, for instance, variability on road friction. The mathematical model results in input-affine nonlinear system. A numerical algorithm based on conjugate gradient method to solve $\mathcal{L}_2$-gain optimal control problem is presented. The proposed algorithm, which has backward-in-time structure, directly finds the feedback control and the "worst case" disturbance variables. Simulations of the controller in closed-loop with the nonlinear vehicle model are shown and discussed.**

I. Introduction

Over the past two decades, there has been tremendous progress in the development of various control strategies for vehicle dynamics stabilization. In [1] and [2] linear $\mathcal{H}_\infty$ controllers that stabilize the vehicle against uncertainty have been proposed. The μ-synthesis has been applied to the linearized vehicle model in [3], obtaining a controller which provides robust stability against perturbations generated in various driving conditions. In [4] a fuzzy-logic controller is proposed to improve vehicle handling and stability when non-linearities are present in the model. A dynamic control allocation approach for vehicle yaw stabilization scheme has been presented in [5]. Also, different model predictive control (MPC) strategies have been explored in the vehicle dynamics context: time-varying MPC [6], [7], hybrid MPC [8], and switched MPC [9].

However, to the knowledge of the authors, the problem of a nonlinear $\mathcal{L}_2$-gain vehicle stability control has not been investigated yet. In this paper, the nonlinear $\mathcal{L}_2$-gain optimal control problem of stabilizing the vehicle dynamics using differential braking and active front steering is considered. We formulate the vehicle dynamics with respect to the tire slip angles. A simplified "magic formula" for the tire model is used. The disturbance (uncertainty) is added on the front and rear cornering forces characteristics. This is a reasonable disturbance, which models, instance, a road friction different of what expected, due to the presence of ice/snow/gravel on the road.

*The work of Vladimir Milić was financed by Croatian Science Foundation. Grant number 03.01/170

**This work was not sponsored by MELCO or any of its subsidiaries.

Vladimir Milić, Josip Kasać and Željko Šitum are with Faculty of Mechanical Engineering and Naval Architecture, University of Zagreb, Zagreb HR-10000, Croatia. Emails: vladimir.milic@fsb.hr, josip.kasac@fsb.hr, zeljko.situm@fsb.hr
Stefano Di Cairano is with Mitsubishi Electric Research Laboratories, Cambridge, MA 02139, USA Email: dicairano@ieee.org
Alberto Bemporad is with IMT (Institutions, Markets, Technologies) Institute for Advanced Studies Lucca, Lucca IT-55100, Italy. Email: alberto.bemporad@imtlucca.it

It is well known [10] that the $\mathcal{L}_2$-gain optimal control problem requires solving a Hamilton-Jacobi-Isaacs equation (HJIE). The analytic solution of HJIE is difficult or impossible to find in most cases. In [11] the HJIE for systems with input constraints is derived. Authors have introduced a two-player policy iteration scheme that results in a framework that allows the use of neural networks to approximate optimal policies and value functions. In [12] an application of neural networks to find a closed-form representation of the feedback strategies and the value function that solves the associated HJIE is presented.

In our approach, the nonlinear $\mathcal{L}_2$-gain optimal control problem is transformed into a nonlinear finite-horizon optimal state feedback control problem with min-max cost. In contrast to the approaches based on neural networks for an approximate solution of HJIE [11], [12], in this paper the tuning of basis functions weights is based on the direct minimization of the performance criterion with respect to the control input, with simultaneous maximization of the same performance criterion with respect to the disturbance. A conjugate gradient approach is used for minimization/maximization of the performance criterion, while the performance criterion gradients are calculated exactly using the chain rule for ordered derivatives. Since the control, disturbance and state variables are treated as dependent variables (coupled via plant equations), the final algorithm has a backward-in-time structure similar to the back-propagation-through-time (BPTT) [13] algorithm.

The algorithm presented in this paper is an extension of the recent work in [14], [15] toward finite-horizon $\mathcal{L}_2$-gain optimal state feedback control. In [14], and [15] a conjugate gradient-based BPTT-like algorithm for optimal open-loop control of nonlinear multivariable systems with control and state constraints is presented. The algorithm performance is illustrated on a realistic high-dimensional vehicle dynamics model. The optimization results have demonstrated favourable features of the algorithm in terms of accuracy, robust numerical stability, and relatively fast execution.

As a further algorithmic improvement, in this work Jacobian matrices are calculated using automatic differentiation (AD). Application of AD comparing with numerical differentiation [15] provide significant reduction of the algorithm computational time.

The rest of the paper is organized as follows. In Section II by formulating the vehicle dynamics using tire slip angles and steering angle as the states and by considering a "magic formula" approximation of the tire forces with respect to the tire slip angles, the mathematical model results in an input-affine nonlinear system. In Section III, the state feedback nonlinear $\mathcal{L}_2$-gain control problem is transformed into a feedback min-max optimal control problem. We formulate the feedback as a linear combination of basis function.

978-1-4673-2066-5/12/$31.00 ©2012 IEEE

The backward-in-time min-max control algorithm is derived. In Section IV the proposed algorithm is implemented to coordinate active front steering and differential braking in a driver-assist steering system that aims at stabilizing the vehicle. Analysis of the simulation results are given. Finally, Section V concludes the paper.

Notation: The notation used is fairly standard. Matrices are represented in bold upper case. All vectors are intended as column vectors and represented in bold lower case. Scalars are represented in italic lower case. The symbol $^{\mathrm{T}}$ denotes transposition, and $\mathbf{0}$ is null matrix of appropriate dimensions. col$(\cdot)$ denotes the operator which puts its arguments into a single column vector and row$(\cdot)$ denotes the operator which puts its arguments into a single row vector. We use diag$(\cdot)$ to denote a diagonal matrix with specified entries on the main diagonal and zeros elsewhere. The derivative of a vector of size m with respect to a vector of size n is a matrix of size $n \times m$. This also means that the derivative of a scalar with respect to a vector is a column vector. The operator $\|\cdot\|$ denotes the Euclidean norm. We avoid to explicitly show the dependence of the variables from the time when not needed.

II. Vehicle yaw stability control

A. Vehicle steering model

This section describes the vehicle model used for control design and simulations. We consider normal "on-road" driving maneuvers, where the vehicle dynamics can be conveniently approximated by the bicycle model [16] shown in Fig. 1. The approximated model has the advantage of reduced complexity over a four-wheel vehicle model, while it is still able to capture the relevant dynamics.

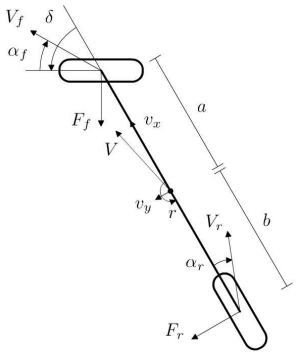

Fig. 1. Schematics of the bicycle model of the vehicle dynamics.

For small steering angles, $\cos\delta \simeq 1$, the vehicle behavior can be described by the differential equations [9]

$$\begin{aligned}
\dot{\alpha}_f &= \frac{F_f + F_r}{m v_x} - \frac{v_x\left(\alpha_f - \alpha_r + \delta\right)}{a+b} + \frac{a\left(aF_f - F_r + Y\right)}{v_x I_z} - \varphi,\\
\dot{\alpha}_r &= \frac{F_f + F_r}{m v_x} - \frac{v_x\left(\alpha_f - \alpha_r + \delta\right)}{a+b} - \frac{b\left(aF_f - F_r + Y\right)}{v_x I_z},\\
\dot{\delta} &= \varphi,
\end{aligned} \tag{1}$$

where α_f [rad] and α_r [rad] are the tire side-slip angles at the front and at the rear tires, respectively, Y [Nm] is the yaw moment obtained by differential braking, φ [rad/s] is the steering angle rate, I_z [kgm^2] is the vehicle inertia along the z-axis, m [kg] is the vehicle mass, a [m] and b [m] are the distances of the front and rear wheel axles from the vehicle center of mass, respectively, v_x [m/s] is the longitudinal velocity at the wheels equal to the one at the center of mass.

The front and rear tire forces F_f [N], F_r [N], respectively, are nonlinear functions of tire slip angles α_f and α_r. In this paper the tire model is based on a simplified form [17] of the "magic formula" [18], i.e.,

$$F_j = \mu D_j \sin\left[C_j \arctan\left(-B_j \alpha_j\right)\right], \tag{2}$$

where $j = f$ for the front tires, and $j = r$ for the rear tires, μ is the tire friction coefficient, B_j, C_j and D_j are tire model parameters. The numerical values of these parameters are given in Section IV. Fig. 2 depicts front and rear tire forces versus side-slip angles for fixed values of the friction coefficients.

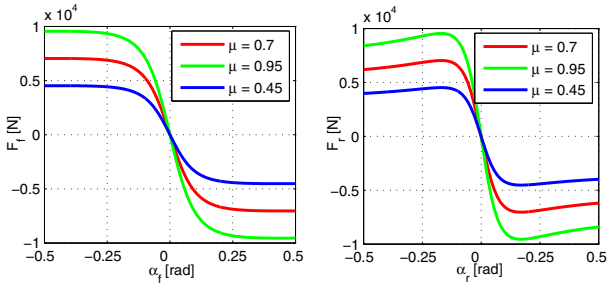

Fig. 2. Tyre force characteristics for different friction coefficient values.

Usually, the major element of uncertainty in the vehicle dynamics is the road friction coefficient μ. We assume its value is within a certain known interval. The variations in the coefficient μ can be represented by $\mu = \overline{\mu}(1+p_\mu \Delta_j)$, where $\overline{\mu}$ is the so-called nominal value of μ, p_μ is the maximum relative uncertainty with $-1 \le \Delta_j \le 1$ being the relative variation. If we choose the disturbance vector components as $d_j = \Delta_j\, \overline{\mu}\, D_j \sin\left[C_j \arctan\left(-B_j \alpha_j\right)\right]$, it follows that

$$F_j = \overline{\mu}\, D_j \sin\left[C_j \arctan\left(-B_j \alpha_j\right)\right] + p_\mu\, d_j. \tag{3}$$

B. Control problem formulation

Let $\mathbf{x} = [x_1\ x_2\ x_3]^{\mathrm{T}} = [\alpha_f\ \alpha_r\ \delta]^{\mathrm{T}}$, $\mathbf{u} = [u_1\ u_2]^{\mathrm{T}} = [Y\ \varphi]^{\mathrm{T}}$ and $\mathbf{d} = [d_1\ d_2]^{\mathrm{T}} = [d_f\ d_r]^{\mathrm{T}}$ be the state, the control input, and the disturbance input of the vehicle dynamics, respectively. With the previously defined vectors, the vehicle model (1), (3) can be easily transformed into a control-oriented affine nonlinear dynamical system.

The control objective is to find control inputs Y (vehicle's yaw moment) and φ (steering angle rate) and to determine the "worst case" disturbance (with respect to the friction coefficient) that avoid the vehicle dynamics (1) to be unstable.

The limits on the braking torques induce constraints on the achievable yaw moment, that, for the maneuvers of interest, are enforced by $-Y_{max} \le Y \le Y_{max}$. In addition, we consider constraints on the steering angle rate $-\varphi_{max} \le \varphi \le \varphi_{max}$.

In order to achieve desired behavior, the following cost function is defined

$$J = \int_0^{t_f} \left(\|\mathbf{z}\|^2 - \gamma^2 \|\mathbf{d}\|^2 + \sum_{k=1}^{4} K_k g_k^2 H^-\left(g_k\right) \right) dt, \tag{4}$$

where $\|\mathbf{z}\|^2 = \mathbf{x}^{\mathrm{T}}\,\mathbf{Q}_x\,\mathbf{x} + \mathbf{u}^{\mathrm{T}}\,\mathbf{Q}_u\,\mathbf{u}$, and g_k are the components of the vector function consisting of control inequality constraints. $\mathbf{Q}_x$ and $\mathbf{Q}_u$ are positive definite weight matrices.

$H^-(\cdot)$ is the Heaviside step function defined as $H^-(\cdot) = 0$ if $(\cdot) \geq 0$, and $H^-(\cdot) = 1$ if $(\cdot) < 0$. Note that although the Heaviside step function $H^-(\cdot)$ is not continuous, the penalty terms of the form $(\cdot)^2 H^-(\cdot)$ in equation (4) are continuously differentiable functions. The penalty function coefficients K_k should be chosen sufficiently large to provide accurate constraints satisfaction.

III. Nonlinear $\mathcal{L}_2$-gain optimal control design

Consider an affine nonlinear dynamical system in the form,

$$\begin{aligned} &\dot{\mathbf{x}}(t) = \mathbf{f}(\mathbf{x}) + \mathbf{G}_1(\mathbf{x})\mathbf{u}(t) + \mathbf{G}_2(\mathbf{x})\mathbf{d}(t),\ \mathbf{x}(0) = \mathbf{x}_0, \\ &\mathbf{z}(t) = \begin{bmatrix} \mathbf{g}_3(\mathbf{x}) \\ \mathbf{u}(t) \end{bmatrix},\ \mathbf{f}(0) = 0,\ \mathbf{g}_3(0) = 0, \end{aligned} \tag{5}$$

where $\mathbf{x} \in \mathbb{R}^{n_0}$ is the state vector, $\mathbf{u} \in \mathbb{R}^{n_u}$ is the control input, $\mathbf{d} \in \mathbb{R}^{n_d}$ is the vector representing internal/external disturbance, $\mathbf{z} \in \mathbb{R}^{n_z}$ is the to-be-controlled output or penalty variable. The functions $\mathbf{f}(\cdot)$, $\mathbf{G}_1(\cdot)$, $\mathbf{G}_2(\cdot)$, $\mathbf{g}_3(\cdot)$ are smooth functions of $\mathbf{x}$. It is assumed that $\mathbf{d} \in \mathcal{L}_2[0,\ t_f]$, $t_f \geq 0$, where $\mathcal{L}_2[0,\ t_f]$ denotes the standard Lebesgue space of vector valued square integrable functions over $[0,\ t_f]$. Note that, the vehicle model (1), (3), is easily formulated as (5).

For the case when all the states of the system are available, the objective is to determine a state-feedback controller $\mathbf{u}(\mathbf{x})$ and determine the "worst case" disturbance internal/external variables $\mathbf{d}(\mathbf{x})$, such that the finite $\mathcal{L}_2$-gain from $\mathbf{d}$ to $\mathbf{z}$ is less than or equal to some positive number $\gamma > 0$. In other words, for every initial condition $\mathbf{x}(0) = \mathbf{x}_0$,

$$\int_0^{t_f} \|\mathbf{z}\|^2 dt \leq \gamma^2 \int_0^{t_f} \|\mathbf{d}\|^2 dt + J(\mathbf{x}_0). \tag{6}$$

The original idea behind this approach is to formulate the $\mathcal{L}_2$-gain optimal control problem as a differential game in which $\mathbf{u}$ and $\mathbf{d}$ are two opposing players [19]. It is well known [20] that this problem is equivalent to solving the min-max optimization problem

$$J^* = \min_{\mathbf{u}} \max_{\mathbf{d}} \left\{ \int_0^{t_f} \left(\|\mathbf{z}\|^2 - \gamma^2 \|\mathbf{d}\|^2 \right) dt \right\} \tag{7}$$

subject to (5).

Problem (7) is solved by the feedback [10]

$$\mathbf{u}^*(\mathbf{x}) = -\mathbf{G}_1^{\mathrm{T}}(\mathbf{x}) \frac{\partial V}{\partial \mathbf{x}}, \quad \mathbf{d}^*(\mathbf{x}) = \frac{1}{\gamma^2} \mathbf{G}_2^{\mathrm{T}}(\mathbf{x}) \frac{\partial V}{\partial \mathbf{x}}, \tag{8}$$

where $V \geq 0$ is the solution of the corresponding HJIE with $V(0) = 0$.

Lemma 1: If *(i)* the nonlinear system (5) is asymptotically stable with $\mathbf{d} = 0$ and $\mathbf{u} = \mathbf{u}^*$, and *(ii)* has $\mathcal{L}_2$-gain less than γ when $\mathbf{d} \neq 0$, and *(iii)* the cost function (7) is smooth, then the closed-loop dynamics are asymptotically stable.

Proof: See [10]. ∎

A. Algorithm derivation

In order to numerically solve problem (7) subject to (5), we consider a special form of $\mathbf{u}$ and $\mathbf{d}$ from (8) as follows

$$\hat{\mathbf{u}}(\mathbf{x}) = \boldsymbol{\Theta}(\mathbf{x})\,\boldsymbol{\pi}(t), \quad \hat{\mathbf{d}}(\mathbf{x}) = \boldsymbol{\Psi}(\mathbf{x})\,\boldsymbol{\rho}(t), \tag{9}$$

where $\boldsymbol{\Theta}(\mathbf{x}) \equiv \operatorname{diag}\left(\boldsymbol{\theta}^1(\mathbf{x}),\ \ldots,\ \boldsymbol{\theta}^{n_u}(\mathbf{x})\right)$ and $\boldsymbol{\Psi}(\mathbf{x}) \equiv \operatorname{diag}\left(\boldsymbol{\psi}^1(\mathbf{x}),\ \ldots,\ \boldsymbol{\psi}^{n_d}(\mathbf{x})\right)$, with $\boldsymbol{\theta}^i(\mathbf{x}) \equiv \operatorname{row}\left(\theta_1^i(\mathbf{x}),\ \ldots,\ \theta_{n_\theta}^i(\mathbf{x})\right)$ and $\boldsymbol{\psi}^i(\mathbf{x}) \equiv \operatorname{row}\left(\psi_1^i(\mathbf{x}),\ \ldots,\ \psi_{n_\psi}^i(\mathbf{x})\right)$ are vectors of basis functions on a compact set $\Omega \subset \mathbb{R}^{n_0}$ with $\theta_j^i(\mathbf{x}) \in C^1(\Omega)$, $\psi_j^i(\mathbf{x}) \in C^1(\Omega)$, and $\theta_j^i(0) = 0$, $\psi_j^i(0) = 0$. Furthermore, $\boldsymbol{\pi}(t) \equiv \operatorname{col}\left(\mathbf{p}^1(t),\ \ldots,\ \mathbf{p}^{n_u}(t)\right)$ and $\boldsymbol{\rho}(t) \equiv \operatorname{col}\left(\mathbf{r}^1(t)\ \ldots,\ \mathbf{r}^{n_d}(t)\right)$, where $\mathbf{p}^i(t) \equiv \operatorname{col}\left(p_1^i(t),\ \ldots,\ p_{n_\theta}^i(t)\right)$ and $\mathbf{r}^i(t) \equiv \operatorname{col}\left(r_1^i(t),\ \ldots,\ r_{n_\psi}^i(t)\right)$, are the vectors of basis functions time-varying weights.

Weierstrass's theorem [21] guarantees that any continuous function on a bounded domain in $\mathbb{R}^{n_0}$ can be approximated by a complete independent basis set. Standard usage of Weierstrass's approximation theorem exploits polynomial basis functions. Non-polynomial basis sets have been considered in [22], where it is shown that linear combination of basis functions with time-varying weights can be used to uniformly approximate continuous time-varying functions.

Hence, with control and disturbance variables from (9), the final min-max optimization problem is

$$J^* = \min_{\boldsymbol{\pi}} \max_{\boldsymbol{\rho}} \left\{ \int_0^{t_f} \left(\|\mathbf{g}_3\|^2 + \mathbf{w}^{\mathrm{T}}\,\mathbf{Q}(\mathbf{x})\,\mathbf{w} \right) dt \right\}, \tag{10}$$

subject to

$$\dot{\mathbf{x}}(t) = \mathbf{f}(\mathbf{x}) + \boldsymbol{\Gamma}(\mathbf{x})\,\mathbf{w}(t),\ \mathbf{x}(0) = \mathbf{x}_0, \tag{11}$$

where $\mathbf{w}(t) \equiv \left[\boldsymbol{\pi}^{\mathrm{T}}(t)\ \ \boldsymbol{\rho}^{\mathrm{T}}(t)\right]^{\mathrm{T}}$, $\boldsymbol{\Gamma}(\mathbf{x}) \equiv [\mathbf{G}_1(\mathbf{x})\,\boldsymbol{\Theta}(\mathbf{x})\ \ \mathbf{G}_2(\mathbf{x})\,\boldsymbol{\Psi}(\mathbf{x})]$ and $\mathbf{Q}(\mathbf{x}) \equiv \begin{bmatrix} \boldsymbol{\Theta}^{\mathrm{T}}(\mathbf{x})\,\boldsymbol{\Theta}(\mathbf{x}) & \mathbf{0} \\ \mathbf{0} & -\gamma^2\,\boldsymbol{\Psi}^{\mathrm{T}}(\mathbf{x})\,\boldsymbol{\Psi}(\mathbf{x}) \end{bmatrix}$.

1) Time discretization: To compute the numerical approximation of the nonlinear $\mathcal{L}_2$-gain optimal control problem, we discretize the system dynamics (11) and the performance criterion (10) basing on the explicit Adams method.

Assume that the time interval $[0,\ t_f]$ is divided into $N-1$ sub-intervals of equal length. Then, the time grid consists of points $t_i = i\tau$ for $i = 0,\ 1,\ 2,\ \ldots,\ N-1$, where $\tau = t_f/N$ is the time step length.

The explicit k-th order Adams method can be conveniently transformed into the following discrete-time state-space form

$$\hat{\mathbf{x}}(i+1) = \hat{\boldsymbol{\phi}}\left(\hat{\mathbf{x}}(i),\ \mathbf{w}(i)\right),\ \ \hat{\mathbf{x}}(0) = \hat{\mathbf{x}}_0, \tag{12}$$

for $i = k-1,\ k,\ k+1,\ \ldots$, and initial conditions $\mathbf{x}(0) = \mathbf{x}_0$, $\mathbf{x}(1) = \mathbf{x}_1,\ \ldots,\ \mathbf{x}(k-1) = \mathbf{x}_{k-1}$ where $\hat{\mathbf{x}}(t)$ is the extended $(n_a = n_0 \cdot k)$-dimensional state vector

$$\hat{\mathbf{x}}(i) = \begin{bmatrix} x_1(i) & x_2(i) & \ldots & x_{n_a-1}(i) & x_{n_a}(i) \end{bmatrix}^{\mathrm{T}}, \tag{13}$$

and

$$\hat{\boldsymbol{\phi}} = \begin{bmatrix} x_1(i) + \tau a_1 \phi_1(i) + \tau x_{n_0+1}(i) & \ldots & a_k \phi_{n_0}(i) \end{bmatrix}^{\mathrm{T}}, \tag{14}$$

where $\boldsymbol{\phi}(\cdot) = \mathbf{f}(\mathbf{x}(\cdot)) + \boldsymbol{\Gamma}(\mathbf{x}(\cdot))\,\mathbf{w}(\cdot)$. $a_1,\ \ldots,\ a_k$ are constant coefficients (for their numerical values see [23]).

Lemma 2: Adams method (12) is convergent if and only if it is stable and consistent.

Proof: See [23, p. 392]. ■

As a multistep method, the Adams method of the k-th order requires the knowledge of k initial conditions. In this work, to determine these initial conditions the fourth-order Runge-Kutta method [23] is used.

The discrete-time form of the performance criterion results in

$$J(\mathbf{x}_0) = \tau \sum_{i=0}^{N-1} F\left(\hat{\mathbf{x}}(i),\, \mathbf{w}(i)\right), \tag{15}$$

where $F(\cdot)$ is the sub-integral function of (10) in the i-th sampling interval.

2) Conjugate gradient algorithm: The numerical algorithm for tuning the $\boldsymbol{\pi}$ weights is based on the direct minimization of the performance criterion with simultaneous tuning of the $\boldsymbol{\rho}$ weights through the maximization of the same performance criterion.

In this work the optimization is performed by a conjugate gradient descent/ascent algorithm in the following form

$$\mathbf{s}^{(l+1)}(i) = -\mathbf{g}^{(l+1)}(i) + \beta^{(l)}\mathbf{s}^{(l)}(i), \tag{16}$$

$$\mathbf{w}^{(l+1)}(i) = \mathbf{w}^{(l)}(i) + \eta^{(l)}\mathbf{s}^{(l)}(i), \tag{17}$$

where $\mathbf{g}(i) \equiv \left(\frac{\partial J}{\partial \mathbf{w}(i)}\right)^{\mathrm{T}} \equiv \left[\left(\frac{\partial J}{\partial \boldsymbol{\pi}(i)}\right)^{\mathrm{T}} \left(-\frac{\partial J}{\partial \boldsymbol{\rho}(i)}\right)^{\mathrm{T}}\right]^{\mathrm{T}}$, for $l = 1, 2, \ldots, M$. M is the number of gradient algorithm iterations, and $\mathbf{s}$ is the search direction vector.

The maximization of the performance criterion with respect to $\boldsymbol{\rho}$ is obtained simply by changing the sign in front of the gradient of the cost function.

The standard method for computing $\eta^{(l)}$ is the line search algorithm which requires one-dimensional minimization of the performance criterion. This is a computationally expensive method which may require many evaluations of the performance criterion during one iteration of the gradient algorithm. Also, if the performance criterion is not appropriately scaled, the line search algorithm may exhibit poor convergence properties [15]. In order to avoid these issues, we use the SuperSAB approach [24] which requires only the information on the gradient directions in two consecutive iterations of the gradient algorithm. The algorithm is modified in terms of using a scalar convergence rate $\eta^{(l)}$ (as oppose to a matrix formulation), in order to avoid discontinuities in vector $\mathbf{w}$. The modified SuperSAB algorithm is given by

$$\eta^{(l)} = \begin{cases} d^{+}\,\eta^{(l-1)} & \text{if} \quad \mathbf{g}^{\mathrm{T}(l)}\,\mathbf{g}^{(l-1)} > 0, \\ d^{-}\,\eta^{(l-1)} & \text{if} \quad \mathbf{g}^{\mathrm{T}(l)}\,\mathbf{g}^{(l-1)} < 0, \\ \eta^{(l-1)} & \text{if} \quad \mathbf{g}^{\mathrm{T}(l)}\,\mathbf{g}^{(l-1)} = 0, \end{cases} \tag{18}$$

where $0 < d^{-} < 1 < d^{+}$ are dilatation coefficients (decreasing/increasing factors).

The scalar $\beta^{(l)}$ is determined by [25]

$$\beta^{(l)} = \frac{\mu \mathbf{g}^{\mathrm{T}(l+1)}\,\mathbf{g}^{(l+1)} + [1-\mu]\mathbf{g}^{\mathrm{T}(l+1)}\left[\mathbf{g}^{(l+1)} - \mathbf{g}^{(l)}\right]}{\nu \mathbf{g}^{\mathrm{T}(l)}\,\mathbf{g}^{(l)} + [1-\nu]\mathbf{s}^{\mathrm{T}(l)}\,[\mathbf{g}^{(l+1)} - \mathbf{g}^{(l)}]}, \tag{19}$$

where $\mu \in [0,\ 1]$ and $\nu \in [0,\ 1]$. If the scalars μ and ν take only their extreme values, 0 or 1, then four possible combinations are obtained: the Fletcher-Reeves method for $\mu = 1$ and $\nu = 1$, the Polak-Ribere method for $\mu = 0$ and $\nu = 1$, the Hestenes-Stiefel method for $\mu = 0$ and $\nu = 0$, the Dai-Yaun method for $\mu = 1$ and $\nu = 0$.

It is important to note that, in order to ensure numerical stability of the algorithm, the parameter $\beta^{(l)}$ is limited to β_{max}. If the parameter $\beta^{(l)}$ has a constant value, $0 < \beta^{(l)} < 1$, then the conjugate gradient algorithm becomes equivalent to a standard gradient algorithm with momentum.

3) Gradient calculation: The gradient of the performance criterion (15) with respect to $\mathbf{w}$ in the l-th iteration of the gradient algorithm is given by

$$\frac{\partial J}{\partial \mathbf{w}(j)} = \tau \sum_{i=0}^{N-1} \frac{\partial F(i)}{\partial \mathbf{w}(j)} = \tau \left(\frac{\partial F(j)}{\partial \mathbf{w}(j)} + \sum_{i=j+1}^{N-1} \frac{\partial F(i)}{\partial \mathbf{w}(j)} \right), \tag{20}$$

for $j = 0,\ 1,\ 2,\ \ldots,\ N-1$, where (because of the causality principle) the terms with $i < j$ are equal to zero.

The terms in the sum on the right-hand side of (20) depend on $\mathbf{w}(j)$ implicitly through $\hat{\mathbf{x}}(i)$ for $i > j$, which gives

$$\frac{\partial F(i)}{\partial \mathbf{w}(j)} = \frac{\partial \hat{\mathbf{x}}(i)}{\partial \mathbf{w}(j)}\, \frac{\partial F(i)}{\partial \hat{\mathbf{x}}(i)}. \tag{21}$$

From (12) it follows that

$$\frac{\partial \hat{\mathbf{x}}(j+1)}{\partial \mathbf{w}(j)} = \frac{\partial \hat{\boldsymbol{\phi}}(j)}{\partial \mathbf{w}(j)},\ \frac{\partial \hat{\mathbf{x}}(i)}{\partial \mathbf{w}(j)} = \frac{\partial \hat{\mathbf{x}}(i-1)}{\partial \mathbf{w}(j)}\, \frac{\partial \hat{\boldsymbol{\phi}}(i-1)}{\partial \hat{\mathbf{x}}(i-1)}, \tag{22}$$

for $i = j+2,\ \ldots,\ N-1$. The above iterative expression is the chain rule for ordered derivatives.

Next, let us denote the second term in the bracket of the right side of equation (20) by $\boldsymbol{\sigma}(j) = \sum_{i=j+1}^{N-1} \frac{\partial F(i)}{\partial \mathbf{w}(j)}$.

Starting from $j = N-2$; $i = N-1$ it follows that

$$\boldsymbol{\sigma}(N-2) = \frac{\partial F(N-1)}{\partial \mathbf{w}(N-2)} = \frac{\partial \hat{\boldsymbol{\phi}}(N-2)}{\partial \mathbf{w}(N-2)}\, \frac{\partial F(N-1)}{\partial \hat{\mathbf{x}}(N-1)}.$$

Further, for $j = N-3$; $i = N-1,\ N-2$ it follows

$$\boldsymbol{\sigma}(N-3) = \frac{\partial F(N-2)}{\partial \mathbf{w}(N-3)} + \frac{\partial F(N-1)}{\partial \mathbf{w}(N-3)} =$$

$$= \frac{\partial \hat{\boldsymbol{\phi}}(N-3)}{\partial \mathbf{w}(N-3)} \left[\frac{\partial F(N-2)}{\partial \hat{\mathbf{x}}(N-2)} + \frac{\partial \hat{\boldsymbol{\phi}}(N-2)}{\partial \hat{\mathbf{x}}(N-2)}\, \frac{\partial F(N-1)}{\partial \hat{\mathbf{x}}(N-1)} \right].$$

This procedure can be further continued for $j = N-4,\ \ldots$ and the final backward-in-time recursive algorithm for calculation of the gradient in (16) has the form

$$\begin{aligned} &\boldsymbol{\omega}(N-1) = \mathbf{0}, \\ &\boldsymbol{\omega}(j) = \frac{\partial F(j+1)}{\partial \hat{\mathbf{x}}(j+1)} + \frac{\partial \hat{\boldsymbol{\phi}}(j+1)}{\partial \hat{\mathbf{x}}(j+1)}\, \boldsymbol{\omega}(j+1), \\ &\boldsymbol{\sigma}(j) = \frac{\partial \hat{\boldsymbol{\phi}}(j)}{\partial \mathbf{w}(j)}\, \boldsymbol{\omega}(j),\ \frac{\partial J}{\partial \mathbf{w}(j)} = \tau \left(\frac{\partial F(j)}{\partial \mathbf{w}(j)} + \boldsymbol{\sigma}(j) \right), \end{aligned} \tag{23}$$

for $j = N-2,\ N-3,\ \ldots,\ 0$. Obviously, from (11) and (12), it follows that $\partial \hat{\boldsymbol{\phi}}(j)/\partial \mathbf{w}(j) = \boldsymbol{\Gamma}^{\mathrm{T}}(\hat{\mathbf{x}}(j))$, and from (10) and (15), it follows that $\partial F(j)/\partial \mathbf{w}(j) = 2\,\mathbf{Q}(\mathbf{x}(j))\,\mathbf{w}(j)$.

4) Jacobians calculation: The extended Jacobian matrix $\partial \hat{\boldsymbol{\phi}}(\cdot)/\partial \hat{\mathbf{x}}(\cdot)$ for the Adams method can be expressed basing on (12) as function of the basic Jacobian matrix $\partial \boldsymbol{\phi}(\cdot)/\partial \mathbf{x}(\cdot)$. Similarly, the gradient of the function in the summation in (15) with respect to the extended state vector is related to the basic gradient.

The basic Jacobian matrix $\partial \boldsymbol{\phi}(\cdot)/\partial \mathbf{x}(\cdot)$ and gradient $\partial F(\cdot)/\partial \mathbf{x}(\cdot)$ can be calculated using AD. AD is now a widely used tool within scientific computing. A variety of tools exist for AD. In this work, TOMLAB/MAD [26] mathematical software is used.

IV. VEHICLE YAW CONTROL APPLICATION

In the previous section we have developed an approach for solving the $\mathcal{L}_2$-gain optimal control problem for general affine nonlinear systems using a conjugate gradient based numerical algorithm with backward-in-time structure. In this section the application of proposed algorithm to the vehicle yaw stability control problem is presented.

The state feedback $\mathcal{L}_2$-gain optimal control strategy for vehicle stability control synthesized by the proposed numerical algorithm was tested in simulation in closed loop with vehicle dynamics model based on (1), which has been validated in experimental vehicle tests in [9]. For the considered passenger vehicle, we have $m = 2050$ kg, $I_z = 3344$ kgm^2, $a = 1.47$ m, $b = 1.43$ m, $v_x = 15$ m/s.

The coefficients of the "magic formula" (2) are chosen as $D_j = 0.5 \cdot m \cdot g$, where $g = 9.81$ m/s^2, $C_f = 1.2$, $B_f = 8.5$, $C_r = 1.5$ and $B_r = 10.2$. We consider the nominal value $\overline{\mu} = 0.7$. It is assumed that the road friction coefficient μ can vary up to $\pm 40\%$ of its nominal value, i.e., $p_\mu = 0.4$ in (3).

The bounds of the actuators are set to $Y_{max} = 1000$ [Nm] and $\varphi_{max} = 0.5$ [rad/s].

Moreover, the control inputs basis functions are chosen as

$$\begin{bmatrix} Y \\ \varphi \end{bmatrix} = \begin{bmatrix} \boldsymbol{\theta}^1(\alpha_f, \alpha_r) & 0 \\ \mathbf{0} & 1 \end{bmatrix} \begin{bmatrix} \mathbf{p}^1(t) \\ p_1^2(t) \end{bmatrix}, \tag{24}$$

where

$$\boldsymbol{\theta}^1(\alpha_f, \alpha_r) = \begin{bmatrix} \alpha_r & \alpha_r^2 & \alpha_f & \alpha_f\alpha_r & \alpha_f\alpha_r^2 & \alpha_f^2 & \alpha_f^2\alpha_r & \alpha_f^2\alpha_r^2 \end{bmatrix},$$

and the disturbance inputs basis functions are chosen as

$$\begin{bmatrix} d_f \\ d_r \end{bmatrix} = \begin{bmatrix} \psi_1^1(\alpha_f) & 0 \\ 0 & \psi_1^2(\alpha_r) \end{bmatrix} \begin{bmatrix} r_1^1(t) \\ r_1^2(t) \end{bmatrix}, \tag{25}$$

where $\psi_1^1(\alpha_f) = \overline{\mu} p_\mu D_f \sin\left[C_f \arctan\left(B_f \alpha_f\right)\right]$ and $\psi_1^2(\alpha_r) = \overline{\mu} p_\mu D_r \sin\left[C_r \arctan\left(B_r \alpha_r\right)\right]$.

The terminal time is $t_f = 3$ sec and the number of time intervals is $N = 3000$ so that the sampling interval is $\tau = 0.001$ sec. The Polak-Ribiere conjugate gradient method is used, and the number of iterations of the gradient algorithm is $M = 1000$. The numerical values of the algorithm parameters are chosen as $d^+ = 1.15$, $d^- = 0.85$, $\eta^{(0)} = 10.0$, $\beta_{max} = 1.0$. The initial basis functions weights are set to zero.

The weighting factors of the cost function (4) are chosen as follows. The state weighting matrix is $\mathbf{Q}_x = \text{diag}\,(1,\ 1,\ 10)$. The weights on inputs are $\mathbf{Q}_u = \text{diag}\left(10^{-6},\ 1\right)$. The penalty function factors are $K_1 = K_2 = 0.5$ and $K_3 = K_4 = 10$, large enough to satisfy control constraints. The scalar value γ^2 is set to 1.

An important point we want to mention here is that the components of control vector (Y and φ) are different in magnitude. This means that a unique convergence rate for all the control variables in the conjugate gradient algorithm could not be effective. Because of this we use a scaling factor for each component of control vector in the conjugate gradient algorithm.

Simulation results are shown in Figures 3-7. It can be seen in Figure 3 that fast stabilization from the initial conditions $\mathbf{x}_0 = [0.15\ \ 0.25\ \ 0]^{\mathrm{T}}$ is achieved. It can be observed from Figure 4 that the proposed controller yields control inputs $|\hat{\mathbf{u}}| \leq \mathbf{u}_{max}$. The basis function weights r_1^1 and r_1^2 of the disturbance inputs d_j are considered as normalized uncertainty term Δ_j of the vehicle dynamics so that $-1 \leq r_1^1,\ r_1^2 \leq 1$ as shown in Figure 5. In Figure 6 time histories of front and rear tire forces are shown.

Furthermore, in a second series of simulation tests we analyzed the robustness to disturbance variations for the case $\mu = \{\text{worst case},\ 0.95,\ 0.45\}$. In Figure 7 it can been seen that the proposed robust optimal controller provides a good degree of robustness, with very limited variability of the trajectories despite large variations in the parameters.

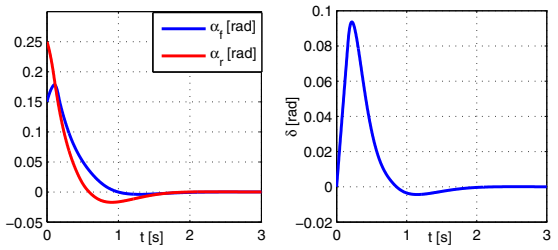

Fig. 3. Time histories of front and rear tire slip angles (left) and steering angle (right).

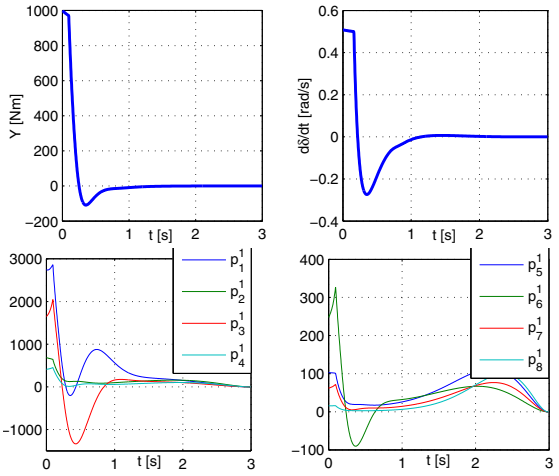

Fig. 4. Time histories of yaw moment, steering angle (upper plots) and basis functions weights (lower plots).

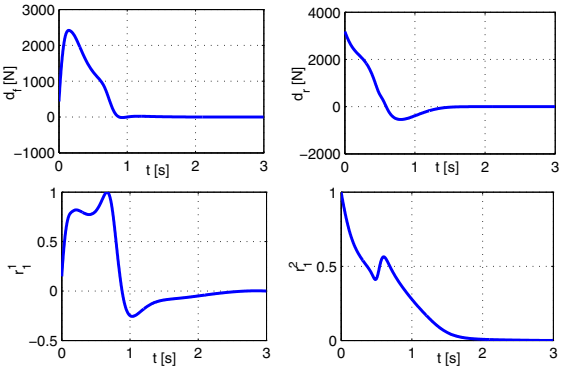

Fig. 5. Time histories of disturbance inputs (upper plots) and basis functions weights (lower plots).

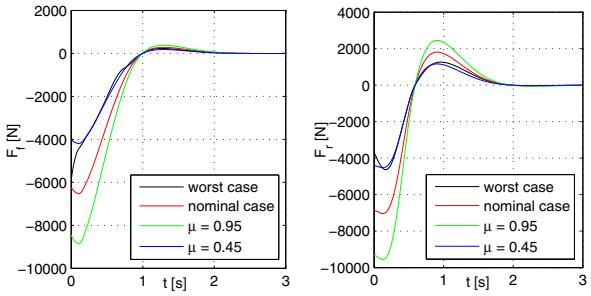

Fig. 6. Time histories of front and rear tire forces.

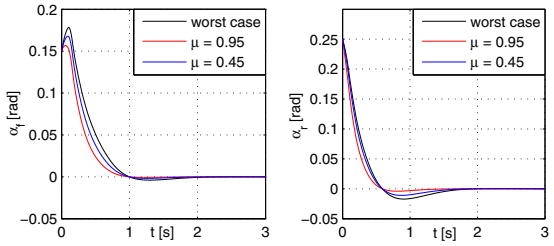

Fig. 7. Time histories of front and rear tire slip angles in the robustness simulations.

V. Conclusion

In this paper the application of a numerical algorithm for $\mathcal{L}_2$-gain vehicle yaw stability control problem has been presented. The proposed algorithm directly finds the control inputs (vehicle's yaw moment and steering angle rate) in the presence of uncertainty in the vehicle dynamics (e.g., in the road friction coefficient) to avoid the vehicle dynamics to become unstable. The closed-loop dynamics response is evaluated in computer simulations, on a model validated in experimental tests in [9].

While the individual methods such as backward-in-time techniques, conjugate gradient optimization algorithms, Adams method for solving ODEs, and AD are known from the literature, in our approach they are integrated together to provide an effective, novel algorithm for numerical solution of the $\mathcal{L}_2$-gain optimal control problems.

Comparison of the algorithm with other existing methods is a subject of ongoing work and future publications. Also, in future work the proposed algorithm for $\mathcal{L}_2$-gain optimal control will be extended with a dynamic observer thus implementing optimal output feedback control. Further improvements of the algorithm application in terms of using a more precise vehicle dynamics model will be considered as well. Indeed the proposed algorithm can be applied to higher-order systems with some increase in complexity.

References

[1] J. H. Park and W. S. Ahn, "$\mathcal{H}_\infty$ yaw-moment control with brakes for improving driving performance and stability," in *Proceedings of the 1999 IEEE/ASME International Conference on Advanced Intelligent Mechatronics*, Atlanta, USA, September 1999, pp. 747–752.

[2] E. Ono, S. Hosoe, H. Tuan, and S. Doi, "Bifurcation in vehicle dynamics and robust front wheel steering control," *IEEE Transactions on Control Systems Technology*, vol. 6, no. 3, pp. 412–420, 1998.

[3] E. Ono, K. Takanami, N. Iwama, Y. Hayashi, Y. Hirano, and Y. Satoh, "Vehicle integrated control for steering and traction systems by μ-synthesis," *Automatica*, vol. 30, no. 11, pp. 1639–1647, 1994.

[4] B. Boada, M. Boada, and V. Diaz, "Fuzzy-logic applied to yaw moment control for vehicle stability," *Vehicle System Dynamics*, vol. 43, no. 10, pp. 753–770, 2005.

[5] J. Tjonnas and T. Johansen, "Stabilization of automotive vehicles using active steering and adaptive brake control allocation," *IEEE Transactions on Control Systems Technology*, vol. 18, no. 3, pp. 545–558, 2010.

[6] P. Falcone, F. Borrelli, J. Asgari, H. E. Tseng, and D. Hrovat, "Predictive active steering control for autonomous vehicle systems," *IEEE Transactions on Control Systems Technology*, vol. 15, no. 3, pp. 566–580, 2007.

[7] P. Falcone, H. E. Tseng, F. Borrelli, J. Asgari, and D. Hrovat, "MPC-based yaw and lateral stabilisation via active front steering and braking," *Vehicle System Dynamics*, vol. 46, no. 1, pp. 611 – 628, 2008.

[8] D. Bernardini, S. Di Cairano, A. Bemporad, and H. Tseng, "Drive-by-wire vehicle stabilization and yaw regulation: a hybrid model predictive control design," in *IEEE Conference on Decision and Control and 28th Chinese Control Conference*, Shanghai, P.R. China, 16-18 Dec. 2009, pp. 7621–7626.

[9] S. Di Cairano and H. Tseng, "Driver-assist steering by active front steering and differential braking: design, implementation and experimental evaluation of a switched model predictive control approach," in *IEEE Conference on Decision and Control*, Atlanta, GA, USA, 15-17 Dec. 2010, pp. 2886–2890.

[10] A. Van Der Schaft, "$\mathcal{L}_2$-gain analysis of nonlinear systems and nonlinear state feedback $\mathcal{H}_\infty$ control," *IEEE Transactions on Automatic Control*, vol. 37, no. 6, pp. 770–784, 1992.

[11] M. Abu-Khalaf, F. L. Lewis, and J. Huang, "Policy iterations on the Hamilton-Jacobi-Isaacs equation for $\mathcal{H}_\infty$ state feedback control with input saturation," *IEEE Transactions on Automatic Control*, vol. 51, no. 12, pp. 1989–1995, 2006.

[12] ——, "Neurodynamic programming and zero-sum games for constrained control systems," *IEEE Transactions on Neural Networks*, vol. 19, no. 7, pp. 1243–1252, 2008.

[13] P. J. Werbos, "Backpropagation through time: What it does and how to do it," in *Proceedings of IEEE*, vol. 78, October 1990, pp. 1550–1560.

[14] J. Kasać, J. Deur, B. Novaković, and I. Kolmanovsky, "A Conjugate Gradient-based BPTT-like Optimal Control Algorithm," in *IEEE International Conference on Control*, Saint Petersburg, Russia, July 8-10 2009.

[15] J. Kasać, J. Deur, B. Novaković, I. Kolmanovsky, and F. Assadian, "A conjugate gradient-based BPTT-like optimal control algorithm with vehicle dynamics control application," *IEEE Transactions on Control Systems Technology*, vol. 19, no. 6, pp. 1587–1595, 2011.

[16] A. Gillespie, *Fundamentals of vehicle dynamics*. Warrendale, Pennsylvania: Society of Automotive Engineers, Inc., 1992.

[17] E. Velenis and P. Tsiotras, "Minimum time vs maximum exit velocity path optimization during cornering," in *IEEE International Symposium on Industrial Electronics*, Dubrovnik, Croatia, June 20-23 2005, pp. 355–360.

[18] E. Bakker, L. Nyborg, and H. B. Pacejka, "Tyre modelling for use in vehicle dynamics studies," *SAE Paper Number: 870421*, 1987.

[19] P. Tsiotras, M. Corless, and M. Rotea, "An $\mathcal{L}_2$ disturbance attenuations solution to the nonlinear benchmark problem," *Int. J. Robust Nonlinear Control*, vol. 8, pp. 311–330, 1998.

[20] T. Basar and P. Bernard, *$\mathcal{H}_\infty$ Optimal Control and Related Minimax Design Problems, Second Edition*. Boston, MA: Birkhuser, 1995.

[21] R. Adams and J. Fournier, *Sobolev Spaces*. New York: Academic Press, 2003.

[22] I. W. Sandberg, "Notes on uniform approximation of time-varying systems on finite time intervals," *IEEE Transactions on Circuits and Systems 1: Fundamental Theory and Applications*, vol. 45, no. 8, pp. 863–865, 1998.

[23] E. Hairer, S. P. Nørsett, and G. Wanner, *Solving Ordinary Differential Equations I - Nonstiff Problems, Second Revised Edition*. Berlin: Springer-Verlag, 2008.

[24] T. Tollenaere, "SuperSAB: Fast adaptive backpropagation with good scaling properties," *Neural Networks*, vol. 3, no. 5, pp. 561–573, 1990.

[25] J. L. Nazareth, *Encyclopedia of Optimization. Second Edition*. Springer, New York, 2009, ch. Conjugate-Gradient Methods, pp. 466–470.

[26] S. A. Forth, "An efficient overloaded implementation of forward mode automatic differentiation in MATLAB," *ACM Transactions on Mathematical Software*, vol. 32, no. 2, pp. 195–222, 2006.